Renewable Energy 35 (2010) 435–442

Contents lists available at ScienceDirect

Renewable Energy

journal homepage: www.elsevier.com/locate/renene

Numerical analysis of the characteristics of vertical axis tidal current turbines

Ye Li*, Sander M. Çalişal

Naval Architecture and Offshore Engineering Laboratory, Department of Mechanical Engineering, The University of British Columbia, 6250 Applied Sciences Ln, Vancouver, BC V6T1Z4, Canada

ARTICLE INFO

Article history:
Received 5 February 2009
Accepted 25 May 2009
Available online 21 June 2009

Keywords:
Tidal current energy
Standard for tidal current turbines
Power output
Torque fluctuation
Induced velocity
Acoustic emission

ABSTRACT

Tidal current is considered to be one of the promising alternative green energy resources. Tidal current turbines are devices used for harnessing tidal current energy. The development of a standard for tidal current turbine design is a very important step in the commercialization of tidal current energy as the tidal current industry is growing rapidly, but no standard for tidal current turbines has been developed yet. In this paper, we present our recent efforts in the numerical simulation of the characteristics (e.g., power output, torque fluctuation, induced velocity, and acoustic emission) of tidal current turbines related to the development of the standard. The relationship between the characteristics and the parameters of an example turbine are extensively discussed and quantified. The findings of this paper are expected to be helpful in developing the standards for tidal current turbines in the near future.

1. Introduction

Tidal current energy has been receiving wide attention for its renewability and small environmental footprint. The primary energy-conversion devices for harnessing energy from tidal current are tidal current turbines, which share the same working principles as wind turbines. Hence, the development of the tidal current energy industry follows that of the wind industry, in which the standardization of wind turbines is one of the most important commercialization milestones. During the process of developing standards for wind turbines, both the International Electrotechnical Commission (IEC) and the International Standardization Organization were involved. In the late 1980s, the IEC created a subcommittee, IEC/TC88, to develop wind turbine standard that covers the performance, safety, and reliability of wind turbines. This standard has been followed by most of the stakeholders. The tidal current energy industry is still in its infancy, but the technologies are evolving rapidly. In 2007, the IEC launched a new subcommittee, IEC/TC114, to develop a standard for ocean energy technologies including tide, wave and in-stream current energy-conversion technologies. After the first IEC/TC114 meeting in Ottawa, Canada in May 2008, IEC/TC114 concluded that its focus in the near future should be on studying the performance, safety, and environmental impact of these technologies.

Numerical simulation has been widely used in developing technology standards for different applications such as wind turbine performance and ship maneuverability. Since 2004, the tidal current energy group at the University of British Columbia (UBC) has been focusing on developing numerical models to simulate the operation of tidal current turbines and unsteady flow conditions, and on designing and testing new turbine prototypes. Several notable results have been reported [1–3]. In order to support IEC/TC114's action in developing standards for tidal current turbines and to evaluate whether UBC's prototype turbines are "good" turbines that will satisfy the future standards, we conducted a numerical analysis of the characteristics of the turbines in terms of their performance and environmental impacts. These efforts are summarized in this paper. The important characteristics of a tidal current turbine (power coefficient, torque fluctuation, wake-induced velocity, and acoustic emission) are identified; then, a numerical model is developed to predict these characteristics. Finally, the relationships between these characteristics and the design parameters are discussed extensively. Additionally, the prototype turbine studied in this paper is a vertical axis turbine.[1]

2. Characteristics of tidal current turbines

Standards for tidal current turbines are expected to consist of a number of criteria quantifying the important characteristics of the

* Corresponding author. Tel.:+1 509 392 9866.
E-mail address: liye2005@gmail.com (Y. Li).

[1] Based on the direction of rotation, tidal current turbines can be classified as vertical axis and horizontal axis tidal current turbines.

0960-1481/$ – see front matter © 2009 Elsevier Ltd. All rights reserved.
doi:10.1016/j.renene.2009.05.024

turbines. In order to identify these characteristics, we review the development of IEC standards for wind turbines since there are similarities in the working principles between tidal current turbines and wind turbines. In the latest IEC standards for wind turbines, many characteristics are included, such as safety, performance, reliability, and environmental impact [4]. Most of these characteristics are applicable to tidal current turbines. However, only the safety of tidal current turbines has been studied [5]. In this paper, we discuss the performance and environmental impact of tidal current turbines. Specifically, we analyze four characteristics of the tidal current turbines: power output, torque, induced velocity and acoustic emission.

Power output is the most important characteristic of a tidal current turbine. It is directly related to annual energy output and energy cost, which are the primary features that concern investors [6]. Usually, investors prefer a turbine with high energy output and low cost. A practical way to achieve such an objective is to increase the maximum power output. Hence, the maximum power output of a turbine and the ability to maintain it are of great interest to both researchers and practitioners.

Torque fluctuates during one revolution of a turbine. Torque fluctuation is directly related to the reliability of the device and the power generation of the device which governs power quality [7–9]. Designers want to make a turbine generate a constant torque so that the vibration of the turbine structure and the hydrodynamic load on the electrical power generator can be minimized. Otherwise, the lifetime of the device will be short due to fatigue, and the varying instantaneous power output will lead to poor power quality. An advanced gearbox and an advanced electric power generator can be used to improve power quality, but this will significantly increase the energy cost. Thus, designers prefer to reduce torque fluctuation by optimally designing a turbine.

The wake of a turbine imposes induced velocity on the turbine. The power output of the turbine is quasi-proportional to the cube of the velocity component seen by the blades. The induced velocity will significantly affect the velocity component seen by the blades. Therefore, the turbine's power output is significantly affected by the wake-induced velocity. In order to improve the power quality of tidal current turbines, designers can modify the geometry of the blades and arms, and/or add auxiliary structure according to the wake-induced velocity. More importantly, the wake-induced velocity disturbs the surrounding flow, which may affect the circulation. The fact that turbines may have a negative impact on ambient environmental fluid has received attentions for several years, since the commercialization of wind turbines. Numerical simulation shows that large numbers of wind turbines may have significant impacts on climate change [10]. Similarly, oceanographers need to know the flow velocity to analyze the changes in ocean flow induced by the operation of tidal current turbines, in order to study their effects on the chemical and biological processes in the ocean and on the potential climate change.

Turbines generate noise while rotating, which is regarded as one of the most important environmental impacts from tidal current turbines as it may pose risk to human beings and animals [11]. Technically, the noise generated by a tidal current turbine can be classified into two categories: (1) hydrodynamic noise, which is generated when the fluctuating hydrodynamic lift acts on the turbine blades and when the unsteady load acts on the shaft, and (2) mechanical noise, which is produced by the gearbox and bearings. The hydrodynamic noise mainly propagates under the surface of water while the mechanical noise propagates above the surface. Practically, it is easier to control mechanical noise than to control hydrodynamic noise. The mechanical noise can be reduced by modifying the gearbox (e.g., by inserting damping materials between the gearbox casing and the top of the power-house module, by modifying the wall structure of the power-house, by lowering the pressure angles of the gears, and/or by replacing the spur gears with helical ones). These methods have been well studied and widely adapted in some marine systems to reduce noise. For example, a helical gear system is used in marine propulsion [12]. Studies on mitigating hydrodynamic noise are rarely reported, as it has military implications. In our research, we study the hydrodynamic noise of tidal current turbines.

3. Numerical method

Previously, only a few numerical methods have been developed to simulate the operation of tidal current turbines such as [13–16], but they all focus on predicting the performance rather than the environmental impacts of tidal current turbines and none of them has been proved to be cost-effective. Recently, Li and Calisal [17] developed a cost-effective numerical method, a discrete vortex method with free-wake structure (DVM-UBC for short), to simulate the motion of underwater structures and the unsteady flow. That paper shows that DVM-UBC can also represent the physics of turbine operation and the fluid flow with improved accuracy. These predictions are validated by comparing the results obtained with DVM-UBC and experimental results, which also suggest that DVM-UBC can be used to predict the power coefficient, torque and wake trajectory of a tidal current turbine. In this section, after reviewing the principles of DVM-UBC and a numerical model for calculating the power coefficient and torque, we develop numerical models for calculating the wake-induced velocity and for predicting the acoustic intensity based on DVM-UBC.

3.1. The principles of DVM-UBC

DVM-UBC is developed based on the traditional discrete vortex method (DVM), a potential flow method proposed by Rosenhead [18]. However, the traditional DVM cannot precisely represent the motion of marine applications due to the viscous effect in these applications [19]. By using perturbation theory, Li and Calisal [17] introduced the viscous effect into the traditional DVM and extended it to DVM-UBC by assuming that the viscous effect is limited to the near field where no-slip boundary conditions exist. In DVM-UBC, Lamb vortices are used to replace potential vortices, which are used in the traditional DVM, and a vortex decay scheme is introduced into the formulation for describing the life cycle of vortices in approximating the physics of the unsteady flow around the turbine. One set of bound vortices is employed to represent the blades, and the other set of free vortices, together with the uniform flow, is used to represent the unsteady wake. Furthermore, DVM-UBC is a time-dependent method. In each time step, it utilizes the relationship between the strength of the free vortex and the induced velocity to approximate the flow and predict the lift, and then uses this relationship together with the viscous effects to predict the drag. The obtained lift and drag are used to calculate instantaneous power. In this study, we follow all the assumptions and procedures given in Li and Calisal [17] in using DVM-UBC.

3.2. Induced velocity

In general, given a vortex filament of an arbitrary shape with a strength Γ and a length l (e.g., a turbine blade), the induced velocity at a given point P (but not on the vortex filament), $\overrightarrow{V}_{iP,l}$, can be obtained by using Biot–Savart's Law, as follows:

$$\overrightarrow{V}_{iP,l} = \frac{\Gamma}{4\pi}\int_{l}\frac{\overrightarrow{r}\times d\overrightarrow{l}}{r^3} \tag{1}$$

where $\vec{r}$ denotes the position vector from a point on the filament to point *P*.

There are three types of vortices: blade-bound vortices, spanwise shed vortices, and trailing edge shed vortices. Numerically, by applying Eq. (1) to all the vortices, the total induced velocity at point *P* can be determined by using the following equation:

$$\vec{V}_{iP} = \sum_i \sum_j \vec{V}_{iPT,i,j} + \sum_i \sum_j \vec{V}_{iPS,i,j} + \sum_i \sum_j \vec{V}_{iPB,i,j} \quad (2)$$

where $\vec{V}_{iPT,i,j}$ denotes the velocity induced by the trailing edge wake vortices shed from blade element i at time step j, $\vec{V}_{iPS,i,j}$ denotes the velocity induced by the spanwise wake vortices shed from the same element at the same time step, and $\vec{V}_{iPB,i,j}$ denotes the velocity induced by blade-bound vortex from the same element at the same time step. Consequently, the wake velocity, $\vec{U}_{VP}$, can be obtained by summing the incoming flow velocity, $\vec{U}_\infty$, and the induced velocity given, as follows:

$$\vec{U}_{VP} = \vec{U}_\infty + \sum_i \sum_j \vec{V}_{iPT,i,j} + \sum_i \sum_j \vec{V}_{iPS,i,j} + \sum_i \sum_j \vec{V}_{iPB,i,j}. \quad (3)$$

In this study, both Eqs. (2) and (3) are nondimensionalized by using the incoming flow velocity as the reference velocity.

3.3. Acoustic intensity

The acoustic emission is quantified by calculating the acoustic intensity. Here, we present the formulation of acoustic intensity, a synthesis of which can be found in many textbooks and reviews, such as [20–25].

Hydrodynamic noise propagates in water in the form of acoustic waves. The intensity of the noise field is defined as the time-average vector product of the local pressure fluctuation, $\tilde{p}$, and the particle velocity, $\tilde{u}$. Mathematically, the noise intensity, I, can be expressed as follows:

$$I = \tilde{p}\tilde{u}. \quad (4)$$

The pressure fluctuation and particle velocity are related by Eq. (5):

$$\tilde{p} = Z\tilde{u} \quad (5)$$

where Z is the acoustic impedance of the medium. In a free acoustic field (without reflecting boundaries and with a homogenous sound velocity), at a distance of several wavelengths from the sound source, the acoustic impedance, Z, can be obtained by multiplying the density of the medium, ρ, and the sound velocity, c, as follows:

$$Z = \rho c. \quad (6)$$

We assume that the sound wave generated by a tidal current turbine is a planar sound wave, and the ocean is assumed to be a free acoustic field. Thus, by plugging Eqs. (5) and (6) into Eq. (4), the noise intensity can be expressed as a function of the particle velocity, as follows:

$$I = \rho c\tilde{u}^2. \quad (7)$$

We then assume that the velocity fluctuation is fully induced by the vortex shedding effect and the incoming flow is along the x direction. Because vortex shedding from the blade is a periodic phenomenon, the particle velocity can be approximated by using Eq. (8) as follows:

$$\tilde{u} \approx \vec{U}_x \quad (8)$$

where $\vec{U}_x$ denotes the x-axis component of the particle velocity.

By substituting Eq. (8) into Eq. (7), we get Eq. (9). Then, the noise intensity can be estimated by using Eq. (9), and its dimensionless format is written as Eq. (10)

$$I \approx \rho c\vec{U}_x^2 \quad (9)$$

$$\hat{I} = I/\rho_w c U_\infty^2. \quad (10)$$

4. Results

In this section, we use the numerical model developed by Li and Calisal [17] to predict the power coefficient and torque of an example tidal current turbine, and use the model developed in Section 3 to predict the wake-induced velocity and the noise emission of the turbine. The example turbine is a three-blade vertical axis tidal current turbine, the blade type is NACA0015, the solidity is 0.375, and the Reynolds number is 160,000. The example turbine mentioned in the following discussion refers to the turbine described here.

4.1. Power output

Fig. 1 shows the power coefficient[2] of the example turbine at different tip speed ratios (TSR). It is noted that the maximum power coefficient is around 48%, and is achieved when the TSR is around 3.8. Although the tidal current velocity is highly predictable and almost constant during a revolution of the turbine, the incoming flow still fluctuates as a result of turbulence and/or for other unexpected reasons. The velocity fluctuation changes the TSR. From the results of our experimental tests in the towing tank at UBC, we noticed that the TSR can vary up to 0.5 within one revolution. Consequently, the power coefficient changes with TSR variation, which leads to the unstable power output. The unstable power output brings challenges to the electric system and the electricity transmission system. Therefore, designers always prefer to let the turbine work at a TSR where the power coefficient is relatively high but fluctuates less. In order to quantify the power fluctuation induced by the TSR variation, we define a new coefficient, C_{Cp}, called power fluctuation coefficient, as the ratio of power coefficient fluctuation to TSR variation, given as follows:

$$C_{Cp} = (C_{P,\max} - C_{P,\min})/0.5 \quad (11)$$

where $C_{P,\max}$ and $C_{P,\min}$ denote the maximum power coefficient and minimum power coefficient, respectively, in the given TSR range (0.5 here). For example, the power fluctuation coefficient is 0.8 when TSR is equal to 3.5, which indicates that this turbine may have a very unstable start.

The power fluctuation coefficient is 0.1 which is achieved when the TSR is between 4.25 and 5.5, which implies that it would be desirable to have the turbine work at a TSR within this range. However, a TSR with a lower power fluctuation coefficient may not provide a high power coefficient. One has to balance the high power coefficient against unstable power output, unless he/she has a perfect angular velocity controller to adjust the angular velocity in real time. In general, from a power output point of view, we suggest having the turbine work at a TSR of around 4.75, where the power coefficient is around 38%. We call this TSR the design TSR. Hence,

[2] Power coefficient is the dimensionless power output.

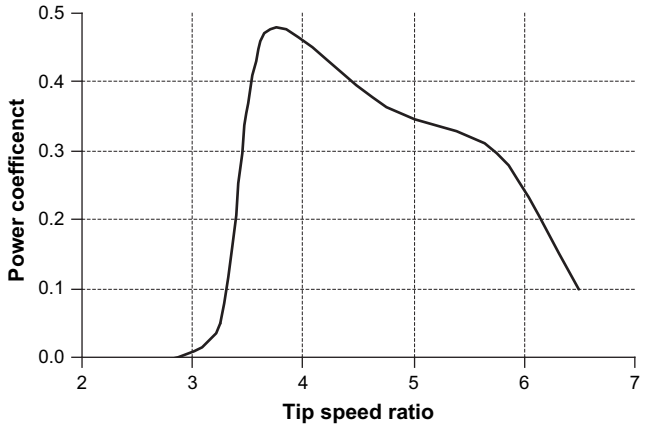

Fig. 1. The relationship between the power coefficient and the tip speed ratio of the example turbine.

we let TSR equal 4.75 in studying the torque, the induced velocity, and the noise emission.

4.2. Torque

Fig. 2 shows a polar diagram of the dimensionless torque of the example turbine and that of an ideal turbine that generates the same power output as the example turbine when the TSR is equal to 4.75. The torque of the ideal turbine is constant, as expected by the mechanical system designers, and thus appears as a circle in the diagram. It is obvious that the torque of the example turbine fluctuates significantly. Thus, the metal fatigue of this turbine's structural components and the fatigue of the generator should be investigated in detail for the purposes of maintaining the reliability.

In order to investigate the variation of the torque systematically, we evaluate the torque output in a frequency domain by using Welch method, which is a method developed by Welch [26] for estimating the spectral density of a random signal in a frequency domain, i.e., power spectrum magnitude (PSM). By using the Welch method, we transform the representation of the results in Fig. 2 (i.e., dimensionless torque vs. azimuth angle) into the representation in Fig. 3 (i.e., power spectrum magnitude of the dimensionless torque vs. dimensionless frequency). For the ideal turbine, it is clear that only one signal (i.e., the DC component) exists as expected. For the example turbine, the first peak represents the power spectrum

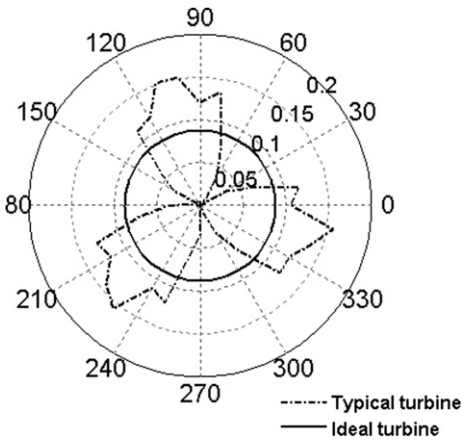

Fig. 2. The relationship between dimensionless torque and the azimuth angle of the example turbine (TSR = 4.75).

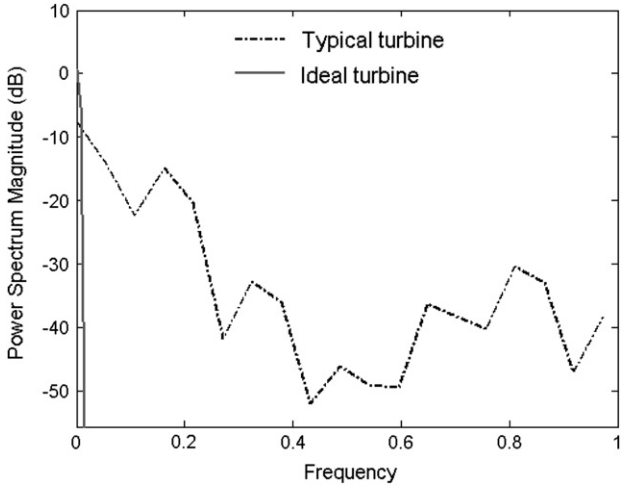

Fig. 3. Dimensionless torque in the frequency domain (TSR = 4.75).

magnitude of the main torque, while the other peaks represent those of the torque fluctuations. If the magnitude of the first peak is much greater than those of the second and third peaks, the torque is more stable. However, the second peak and even the third, fourth and fifth peaks are very close to the first peak here, which suggests that the torque is quite unstable. In order to quantify the torque fluctuation, we define a new dimensionless coefficient, torque fluctuation coefficient, as the partial differential of the power spectrum magnitude with respect to the frequency, as follows:

$$C_{\mathrm{TF}} = \{\Delta T_{\mathrm{peak}}/\Delta f_{\mathrm{peak}} : \text{first five peaks}\} \tag{12}$$

where T_{peak} and f_{peak} denote the torque PSM and the frequency, respectively; ΔT_{peak} and Δf_{peak} denote the change in T_{peak} and the change in f_{peak}, respectively. Thus, it is clear that the larger the C_{TF} is, the more stable the torque is. By using Eq. (12), we get $C_{\mathrm{TF}}[\text{example}] = 38dBS$ and $C_{\mathrm{TF}}[\text{ideal}] \to \infty$.

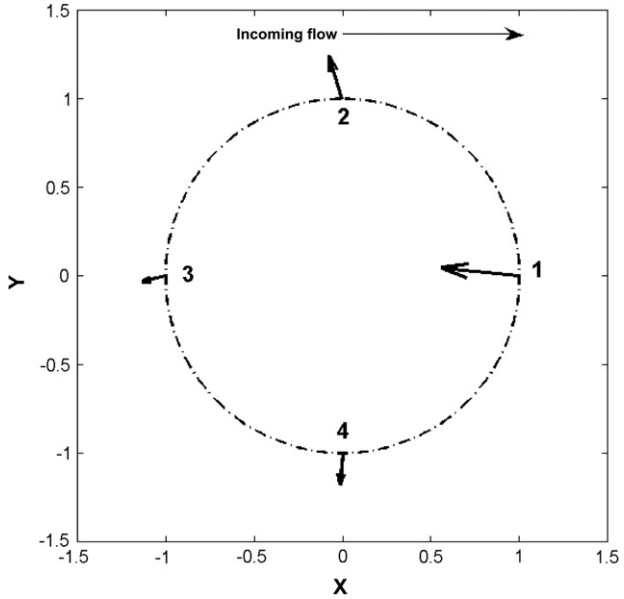

Fig. 4. Dimensionless induced velocity at four points on the example turbine (TSR = 4.75).

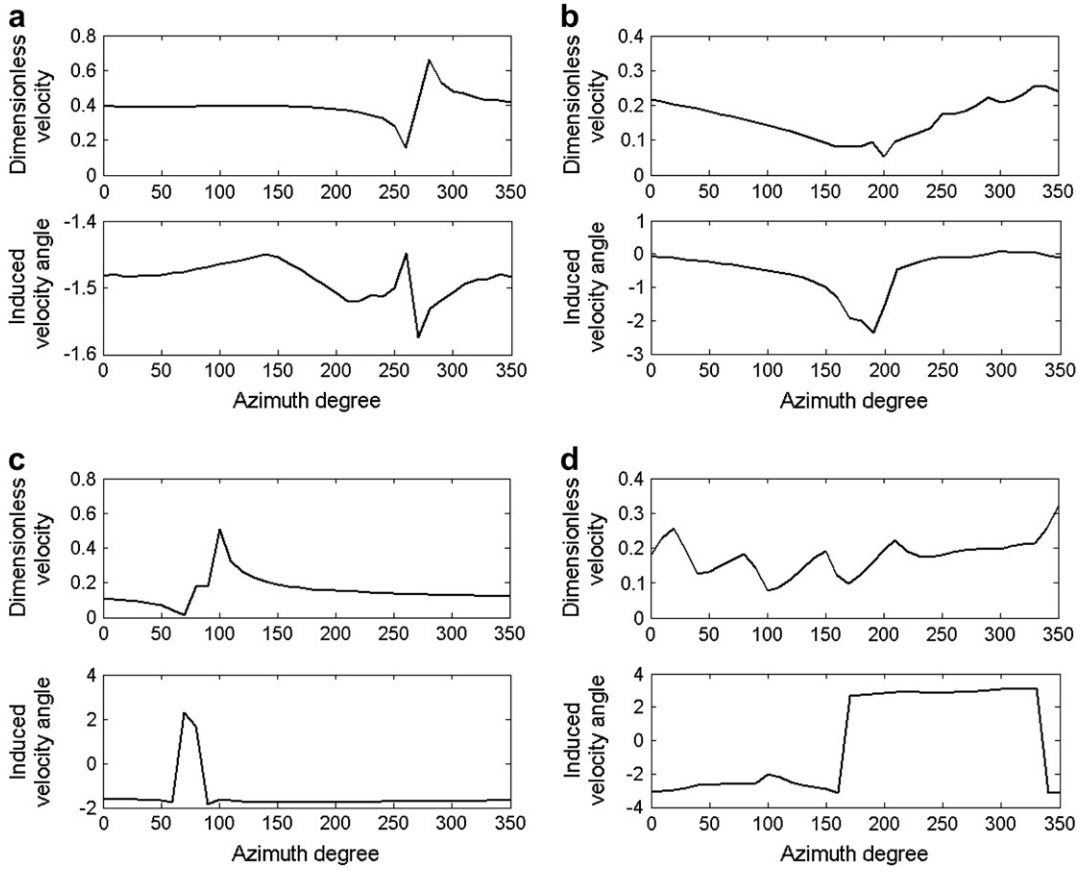

Fig. 5. Dimensionless induced velocity and induced velocity angle at four points on the example turbine (TSR = 4.75): (a) at Point 1; (b) at Point 2; (c) at Point 3; and (d) at Point 4.

4.3. Wake-induced velocity

We examine the induced velocities at four special points on the turbine, the coordinates of which are (1,0), (0,1), (−1,0) and (0,−1), and the coordinates of the shaft of the turbine is (0,0). Fig. 4 shows the dimensionless induced velocities at these four special points just after the turbine finishes one revolution. One may notice the agreement between the induced velocity and the torque. The induced velocity at Point 1 is the largest because Point 1 is located at the center of the downstream area of the turbine, where the torque of the turbine is at around its peak value. The induced velocity at Point 3 is the smallest because Point 3 is located at the center of the upstream area of the turbine, where the torque is at around its trough value (where the azimuth angle is equal to 270°, see Fig. 2). Additionally, crossing flows are observed at both Point 2 and Point 4, which are consistent with the results generated by using Fluent as presented in Nabavi [27].

In order to investigate the dimensionless induced velocities systematically, we analyze their magnitudes and directions in a time sequence during one revolution (i.e., when the azimuth angle varies from 0° to 360°). The results are shown in Fig. 5. The direction of the induced velocity is defined as follows:

$$\theta = \arctan V_{p,x}/V_{p,y} \tag{13}$$

where $V_{p,x}$ and $V_{p,y}$ denote the induced velocities at a given point in the x direction and y direction, respectively.

It is noted in Fig. 5 that (1) at Point 1, both the dimensionless induced velocity and the induced velocity angle are almost constant, except that there is a dramatic change when the azimuth angle is between 250° and 300°; (2) at Point 2, the maximum values of both the dimensionless induced velocity and the induced velocity angle are obtained when the azimuth angle is around 0°, and the minimum values are obtained when the azimuth angle is around 200°; (3) at Point 3, the magnitude of the dimensionless induced velocity remains to be 0 except when the azimuth angle is 100° where the induced velocity is about 0.5. The induced velocity angle remains to be −2 except when the azimuth angle is 75°, where the induced velocity angle is around 2; and (4) at Point 4, the dimensionless induced velocity fluctuates as the azimuth angle changes, with an average induced velocity of around 0.2. The dimensionless induced velocity angle remains to be −3 when the azimuth angle is between 0° and 160° and between 340° and 360° while it remains to be 3 when the azimuth angle is between 160° and 340°. Additionally, the dimensionless induced velocities at Point 2 and Point 4 are both around 0.2, while their temporal variation patterns are different, which shows the asymmetry of the wake.

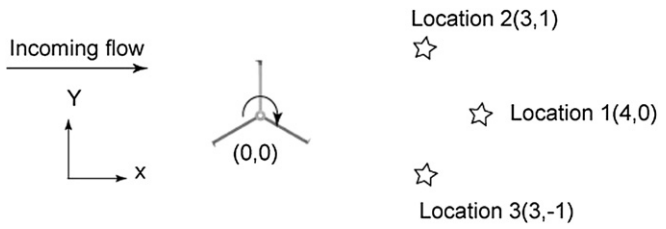

Fig. 6. Locations of the three receivers around the example turbine.

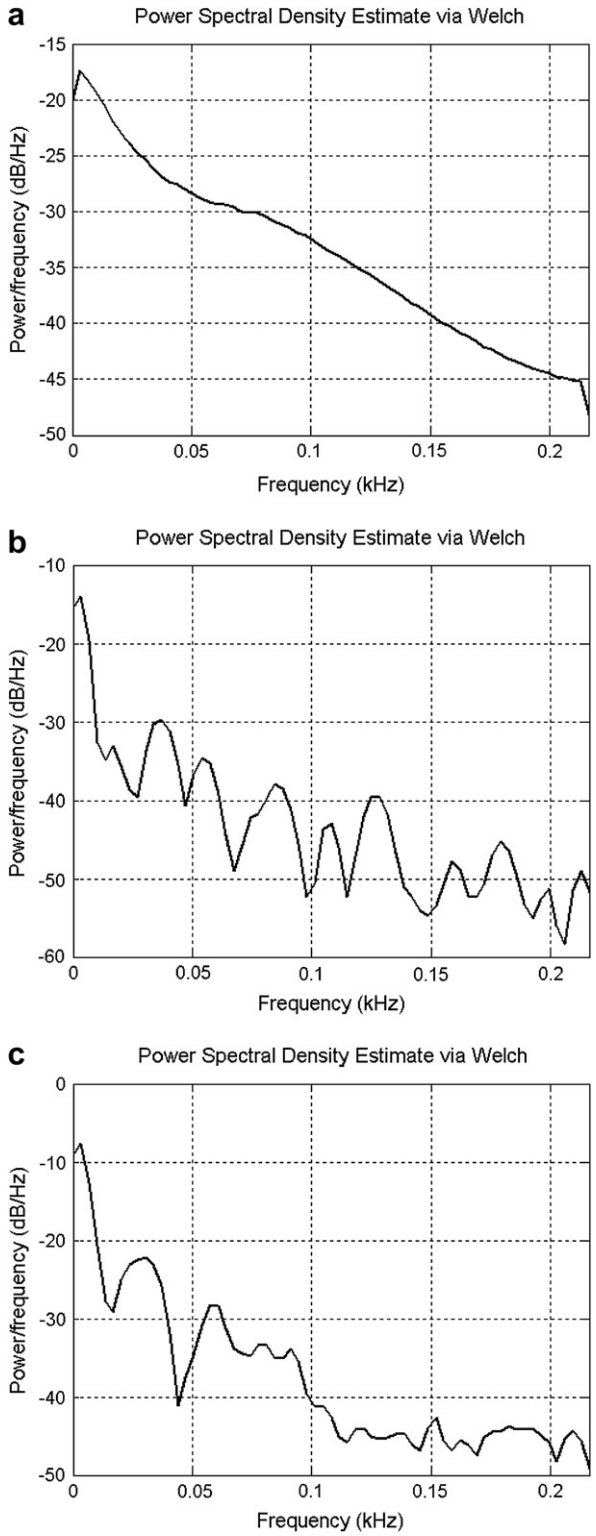

Fig. 7. Power spectrum of the intensity of the noise generated by the example turbine at the three locations: (a) Location 1(4,0); (b) Location 2 (3,1), and (c) Location 3 (3,−1).

4.4. Noise emission

We evaluate the hydrodynamic noise intensity at three locations downstream to the example turbine, as shown in Fig. 6. Assuming that the dimensionless coordinates of the turbine shaft are (0,0) and the incoming flow direction is along the *x*-axis, the dimensionless coordinates of those three receiver locations are (4,0), (3,1), and (3,−1), respectively. One can use these results to analyze not only the noise intensity but also the symmetry of the noise emission from the turbine.

Similar to our evaluation of the torque fluctuation, we use the Welch method to evaluate the magnitude of the noise intensity. It is noted that the frequencies corresponding to the first peak (main noise frequency) at the three locations are all around 4 Hz (Fig. 7). Particularly, the noise intensity at Location 1 only has one peak, which corresponds to a frequency of 4 Hz, while there are multiple peaks at the remaining two locations. For example, the second peak at Location 2 corresponds to a noise frequency of 18 Hz and the second peak at Location 3 corresponds to a noise frequency of 31 Hz. The noise intensity at Locations 2 and 3 are higher than that at Location 1.

Table 1
Fish acoustic information.

Fish name	Sensitive frequency (Hz)
American eel	75
Atlantic herring	30–1200
Atlantic thread herring	1200
Banded rudderfish	60–1000
Bar jack	30
Bigeye mojarra	75–1000
Bigeye scad	50–3000
Bluefish	60–1200
Coney	75
Cownose ray	150

5. Discussion

The numerical models used for analyzing the characteristics of tidal current turbines neglect the shaft and arm effect. Such a simplification is expected to affect the accuracy of the predicted power coefficients and torques somewhat. Research [28] shows, however, that the consequence is acceptable and that the shaft and arm effect on wake velocity fluctuation can be significantly reduced if auxiliary structures are used. Nonetheless, the arm and shaft also have effect on the noise intensity. During one revolution, the blade imposes a strike on the shaft when the blade and the shaft are in a line parallel with the incoming flow, which generates a noise. Its frequency,f_B, can be estimated by using Eq. (14).

$$f_B = n_B\omega/2\pi \tag{14}$$

where $n_B$denotes the number of blades.

Additionally, one may note that the frequency in the analysis above just represents the main noise frequency of the example turbine. The main noise frequency may change as the turbine design changes. Despite the simplification of this model, it is helpful for identifying the noise that might interfere with the communication of those marine animals that are sensitive to these noise frequency bands (see Appendix).

6. Conclusion and future work

This paper presents a preliminary study on the characteristics (power output, torque, induced velocity, and acoustic emission) of a tidal current turbine. Numerical models are used and developed to predict these characteristics for tidal current turbines, and can be used to facilitate the development of standards for tidal current turbines. Besides the well-studied power coefficient, we introduce the power fluctuation coefficient, the torque fluctuation coefficient, the induced velocity angle, and the noise intensity of tidal current

turbines. For a turbine, a high power coefficient is desired along with a low power fluctuation coefficient. From a cost-efficiency point of view, one wants to find an optimal design TSR that balances the high power coefficient against a low fluctuation coefficient, possibly with the assistance of a precise angular velocity controller. Furthermore, the torque fluctuation coefficient should also be high enough to reduce the burden on the electric power generator and increase the reliability of the turbine. During the UBC towing experiment, we found that using auxiliary structures can significantly reduce the torque fluctuation, and that the auxiliary structure can be designed by studying the induced velocity.

This study identifies four different characteristics of the turbine, which can be used to develop standards for tidal current turbines. In the near future, the critical values of these characteristics should be determined. More experimental tests are required to identify these critical values.

Acknowledgements

The authors would like to thank the following agencies for providing fellowships to Ye Li to conduct this research: the University of British Columbia, National Science and Engineering Research Council of Canada, Society of Naval Architects and Marine Engineers, IEEE, American Society of Mechanical Engineers, and the International Society of Offshore and Polar Engineers. We thank Dr. Murray Hodgson for his instructive comments on acoustic emissions, Mr. Craig Wilson for his careful edit of the manuscript, Dr. Daniel Pauly for drawing our attention to his fish database and Dr. Hakan Westerberg for his fruitful discussion on marine mammals' reaction to noise.

Appendix

The direct victims of turbine noise are those marine animals that communicate in the turbine noise frequency bands. As biology is not the focus of this study, we just review the previous research to survey the hearing ability of some marine animals. The description below is a review of papers by marine biologists such as Au [29], Payne and Webb [30], Stafford et al. [31], Wahlberg and Westerberg [32] and Madsen et al. [33]. In particular, Wahlberg and Westerberg [32] and Madsen et al. [33] reviewed the hearing ability of fishes and marine mammals with an emphasis on those sensitive to the band of the noise generated by offshore wind turbines. The main frequency of the noise generated from tidal current turbines is lower than that of the noise generated by wind turbines. Thus, in studying the interference of tidal current turbine noise with marine animals' communication, we focus on those animals that are sensitive to low frequency noise.

Among the marine mammals, large baleen whales generate low frequency, long-duration and powerful calls that in some cases have ocean-traversing potential (Payne and Webb [30]; Stafford et al. [31]). Toothed whales generate short ultrasonic transients (clicks) for navigation and echolocation of prey within the range of tens to hundreds of meters (Au [29]). These whales use low frequency underwater signals (10 ~ 10,000 Hz) for communication and navigation, whereas toothed whales produce sound for echolocation and communication in the frequency range of 1 ~ 150,000 Hz, and pinnipeds communicate by vocalizing with a frequency of about 50 ~ 60,000 Hz (Richardson et al. [34]). In general, baleen whales are more sensitive to low frequency signals while toothed whales are very insensitive to low frequency signals, although most marine animals can be affected by low frequency noise (Madsen [35]). Froese and Pauly [36] summarized fish acoustic information, part of which is shown in Table 1. Marine animals affected by the acoustic emission of a tidal current turbine farm, may have to increase their pitch or change frequency to communicate with each other [37].

References

[1] Li Y., Lence B.J., Calisal S.M. Cost estimation of an in-stream turbine farm system. Journal of Computers 2009; 4(4):288–294.
[2] Li Y., Calisal S.M. Vertical axis tidal turbines with improved efficiency US patent filed on June 28, 2008.
[3] Li Y., Nabavi Y., Alidadi M., Klaptocz V.R., Rawlings G.B., Calisal S.M. Numerical simulation investigation of vertical axis tidal turbines at UBC: RANS CFD and potential flow. The 17th International Offshore and Polar Engineering Conference, July 1–6, 2007 Lisbon, Portugal.
[4] IEC. International standard for wind turbine design. Geneva, Switzerland: International Electrotechnical Commission (IEC); March 2005.
[5] DNV. Certification of tidal and wave energy converters. Oslo, Norway: Det Norske Veritas (DNV); Oct 2008.
[6] Campell C. Industries' reaction to energy cost estimation based on simplified hydrodynamic assumptions. Personal communication, Sept. 2006.
[7] Manwell J., Jeffries W., McGowan J. Power fluctuation from a horizontal axis wind turbine ASME 14th Energy Source Technology Conference, Houston, TX, Jan 20–23, 1991, pp. 63–69.
[8] Takata G, Katayama N, Miyaku M, Nanahara T. Study on power fluctuation characteristics of wind energy converters with fluctuating turbine torque. Electric Engineering in Japan 2005;135(4):1231–9.
[9] Wakui T, Yokoyama R. A suitable load control method for constant tip speed ratio operation of stand-alone wind turbine-generator systems. Wind Engineering 2007;31(1):43–58.
[10] Keith DW, DeCarolis JF, Denkenberger DC, Lenschow DH, Malyshev SL, Pacala S, et al. The influence of large-scale wind-power on global climate. Proceedings of the National Academy of Sciences of the United States 2004;101:16115–20.
[11] Shepherd KP, Grosveld FW, Stephens DG. Evaluation of human exposure to the noise from large wind turbine generators. Noise Control Engineering Journal 1983;21(1):30–7.
[12] Hoppe F., Vollmer B. Advanced propulsion gears for large yachts. The 2nd International Conference on Marine Research and Transportation 2007; Naples, Italy.
[13] Berg D.E. An improved double-multiple streamtube model for the Darrieus-type vertical axis wind turbine. Presentend at The Sixth Biennial Wind Energy, 1983.
[14] Jiang D, Coton FN, Galbraith McD RA. Fixed wake vortex model for vertical axis wind turbines including unsteady aerodynamics. Wind Engineering 1991;15(6):348–60.
[15] Strickland JH, Webster BT, Nguyen T. Vortex model of the Darrieus turbine: an analytical and experimental study. Journal of Fluids Engineering 1979;101:500–5.
[16] Oler JW. Discrete local circulation method for vertical and horizontal axis wind turbines, vol. 11. American Society of Mechanical Engineers, Solar Energy Division; 1991. 41–47.
[17] Li Y., Calisal S.M. Preliminary results of a discrete vortex method for individual marine current turbine. The 26th ASME International Conference on Offshore Mechanics and Arctic Engineering, June 10–15, 2007, San Diego, CA.
[18] Rosenhead L. Formation of vortices from a surface of discontinuity. Proceedings of the Royal Society, London Series A 1931;134:170–92.
[19] Wong H. Slender ship procedures that include the effects of yaw, vortex shedding and density stratification. Doctoral thesis. Department of Mechanical Engineering, the University of British Columbia; 1995.
[20] Beranek LL. Acoustics. New York: Acoustical Society of America; 1983.
[21] Urick RJ. Principles of underwater sound. 3rd ed. New York: McGraw-Hill; 1983.
[22] Kalmijn AD. Hydrodynamic and acoustic field detection. In: Atema J, Fay RR, Popper AN, Tavolga WN, editors. Sensory biology of aquatic animals. New York: Springer-Verlag; 1988. p. 83–131.
[23] Kalmijn AD. Functional evolution of lateral line and inner ear sensory systems. In: Coombs S, Görner P, Münz H, editors. The mechanosensory lateral line: neurobiology and evolution. New York: Springer-Verlag; 1989. p. 187–215.
[24] Burdic WS. Underwater acoustic system analysis. Baileys Harbor, Wisconsin, USA: Peninsula Publishing; 2003.
[25] Etter P. Underwater acoustics modeling and simulation: principles, techniques and applications. London, UK: Taylor & Francis Press; 2003.
[26] Welch D. The use of fast Fourier transform for the estimation of power spectra: a method based on time averaging over short, modified periodograms. IEEE Transactions on Audio Electroacoustics 1967;15(2):70–3.
[27] Nabavi Y. Numerical study of the duct shape effect on the performance of a ducted vertical axis tidal turbine. Master thesis. Department of Mechanical Engineering, the University of British Columbia; 2008.
[28] Li Y. Development of a procedure for predicting the power output from a tidal current turbine farm. PhD dissertation. Department of Mechanical Engineering, the University of British Columbia; 2008.
[29] Au WWL. The sonar of dolphins. New York: Springer-Verlag; 1993.
[30] Payne R, Webb D. Orientation by means of long range acoustic signaling in baleen whales. Annals of the New York Academy of Sciences 1971;188:110–41.

[31] Stafford KM, Fox CG, Clark DS. Long-range acoustic detection and localization of blue whale calls in the northeast Pacific Ocean. Journal of the Acoustical Society of America 1998;104(6):3616–25.
[32] Wahlberg M, Westerberg H. Hearing in fish and their reactions to sounds from offshore wind farms. Marine Ecology Progress Series 2005;288:295–309.
[33] Madsen PT, Wahlberg M, Tougaard J, Lucke K, Tyack P. Wind turbine underwater noise and marine mammals: implications of current knowledge and data needs. Marine Ecology Progress Series 2006;309:279–95.
[34] Richardson WJ, Greene CR, Malme CI, Thompson DH. Marine mammals and noise. San Diego: Academic Press; 1995.
[35] Madsen P.T. Marine animal's hearing to low frequency noise. Personal communication, June 2007.
[36] Froese R, Pauly D. FishBase. Edition 01/2008. Available at: <http://www.fishbase.org> [accessed 03.03.08].
[37] Pauly D. Fish response to high pitch signal in their communication band. Personal Communication, March 3, 2008.